TẠP CHÍ KHOA HỌC
TRƯỜNG ĐẠI HỌC SƯ PHẠM TP HỒ CHÍ MINH
Tập 18, Số 12 (2021): 2124-2137
Website: http://journal.hcmue.edu.vn
ISSN: 2734-9918

HO CHI MINH CITY UNIVERSITY OF EDUCATION
JOURNAL OF SCIENCE
Vol. 18, No. 12 (2021): 2124-2137
https://doi.org/10.54607/hcmue.js.18.12.3277(2021)

Research Article

CALCULATION OF SCATTERING WAVE FUNCTIONS FOR METASTABLE STATES OF A DIATOMIC BERYLLIUM MOLECULE

Luong Le Hai[1*], Nguyen Minh Nhut[1], Luu Kim Lien[1], Gusev Alexander Alexandrovich[2]

[1]Ho Chi Minh City University of Education, Vietnam

[2]Joint Institute for Nuclear Research – Dubna City, Moscow region, Russian Federation

[*]Corresponding author: Luong Le Hai – Email: haill@hcmue.edu.vn

Received: September 23, 2021; Revised: November 09, 2021; Accepted: December 08, 2021

ABSTRACT

In this paper, the computational scheme and calculation results of scattering functions for metastable states of a diatomic beryllium molecule in laser spectroscopy are presented. The solution to the problem is performed using the authors' software package with the high-accuracy finite element method. The procedure of matching tabulated potential functions with van der Waals asymptotic potential using Hermite interpolation polynomials which provides continuity of both the function itself and its derivative is presented. The efficiency of the proposed approach is demonstrated by the spectrum of rotational-vibrational metastable states with complex-valued energy eigenvalues in the diatomic beryllium molecule. For selected metastable states, the corresponding scattering states with real-values resonance energies are calculated and shown in graphs.

Keywords: diatomic beryllium molecule; finite element method; KANTBP 4M program; metastable states; scattering problem

1. Introduction

The vibration-rotational spectrum of diatomic beryllium molecule was studied earlier (Gusev et al., 2019). During the last decade, the theoretical investigations (Lesiuk et al., 2019; Meshkov et al., 2014; Mitin, 2011, 2017; Patkowski et al., 2009) have shown 12 vibrational bound states in a diatomic beryllium molecule, whereas 11 states were extracted from the experimental data of laser pump-probe spectroscopy (Merritt et al., 2009). The boundary value problem (BVP) for the second-order ordinary differential equation (SOODE) with potential function numerically tabulated on a non-uniform grid in a finite interval of the independent variable values was solved (Mitin, 2017). To formulate the BVP on a semiaxis, it is suggested to further explore its potential function beyond the finite interval using the additional information about the interaction of atoms comprising the diatomic molecule at large interatomic distances. The leading term of the potential function at large distances is given by the van der Waals interaction, inversely proportional to the sixth power of the independent variable with the constant, determined from theory (Porsev

Cite this article as: Luong Le Hai, Nguyen Minh Nhut, Luu Kim Lien, & Gusev Alexander Alexandrovich (2021). Calculation of scattering wave functions for metastable states of a diatomic beryllium molecule. *Ho Chi Minh City University of Education Journal of Science, 18*(12), 2124-2137.

& Derevianko, 2006; Sheng et al., 2013). Proceeding in this way we faced a problem of how to match the asymptotic expansion of the potential function with its tabulated numerical values (within the accuracy of their calculation) at a suitable sufficiently large distance.

In the present work, we continue studying these problems and expand our calculating results in previous works by Derbov (2020, 2021) and Gusev (2019, 2021). Firstly, we formulate the quantum scattering problem of diatomic beryllium molecule in which the matching tabulated potential functions with van der Waals asymptotic potential using HIPs which provides continuity of both the function itself and its derivative is presented. Next, we presentthe algorithm for calculating the scattering wave of metastable states in KANTBP 4M program (Gusev et al., 2015). This program solves BVPs of mathematical models reduced from low-dimensional complex quantum models based on the finite element method (FEM) with Hermite interpolation polynomials (HIPs). Finally, by using KANTBP 4M program, the calculation results are presented in graph and table. In the conclusion, we discuss further applications of the elaborated method and results.

2. Problem statement

2.1. Quantum scattering problem of diatomic beryllium molecule

In quantum chemical calculations, effective potentials of interatomic interaction are presented in the form of numerical tables calculated with limited accuracy and defined on a nonuniform mesh of nodes in a finite range of interatomic distances.

The Schrödinger equation for a diatomic molecule in the adiabatic approximation (in which the diagonal nonadiabatic correction is not taken into account), commonly referred to as Born–Oppenheimer (BO) approximation, has the form

$$\left[-\frac{\hbar^2}{2mDa\mathrm{A}^2}\left(\frac{1}{r^2}\frac{d}{dr}r^2\frac{d}{dr}\right)+V_L(r)-E\right]\Phi_L(r)=0, \tag{1}$$

$$V_L(r)=V(r)+\frac{\hbar^2}{2mDa\mathrm{A}^2}\frac{L(L+1)}{r^2}.$$

where L is the total angular momentum quantum number, r is the distance between the atoms in angstroms (A), and $m=M/2=4,506$ is the reduced mass of beryllium molecule.

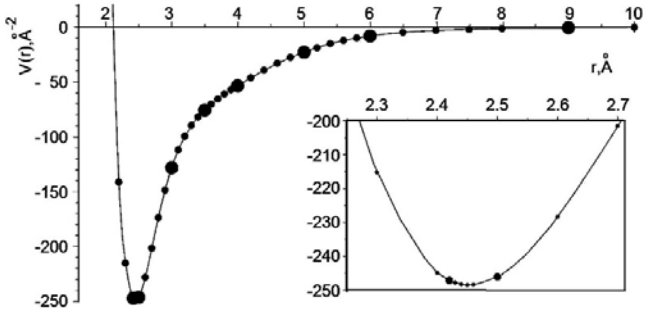

Fig.1. *Potential V(r)(A^{-2}) of the beryllium dimer as a function of r(A) obtained by interpolating the tabulated values (points in the subintervals, the boundaries of which are shown by larger size circles) by fifth-order LIPs*

$Da = 9{,}10938356.10^{-31}\text{kg} = 931{,}494061\text{MeV}$ is the Dalton (atomic mass unit) (NIST), E is the energy in cm^{-1} and $V(r)$ is potential energy curves at $L = 0$, the potential energy curve $U(r) = \left(\frac{2mDa\text{A}^2}{\hbar^2}\right)V(r)$ in A^{-2}, the desired energy $\mathcal{E} = \left(\frac{2mDa\text{A}^2}{\hbar^2}\right)E$ in A^{-2}, i.e. $V(r) = s_2 U(r)\,\text{cm}^{-1}$ and $E = s_2\mathcal{E}\,\text{cm}^{-1}$, where $s_2 = 1/0{,}2672973729$ is the conversion factor from A^{-2} to cm^{-1}.

In Eq. (1) the potential $V(r)$ (in cm^{-1}) (see Fig. 1) is given by the BO potential function marked as the modified expanded Morse oscillator (MEMO) tabular values $\{V^M(r_i)\}_{i=1}^{76}$ in the interval $r \in [r_1 = 1.5, r_{76} = 48]\text{A}$ (Mitin, 2017). These tabular values were chosen to provide a better approximation of the potential $V(r)$ by the fifth-order Lagrange interpolation polynomials (LIPs) of the variable r in subintervals. Indeed, Fig. 2 displays smooth approximation till $r_{49} = 12$ where the approximate potential curve coincides with and crosses the asymptotic potential $V_{as}(r)$ given analytically by the expansions (Porsev & Derevianko, 2006)

$$V_{as}(r) = s_1.\tilde{V}_{as}(r), \quad \tilde{V}_{as}(r) = -(214(3)\text{Z}^{-6} + 10230(60)\text{Z}^{-8} + 504300\text{Z}^{-10}), \tag{2}$$

where $s_1 = 58664{,}99239$ is the conversion factor from aue to A^{-2}, $Z = r/s_3$ and $s_3 = 0{,}52917$ is Bohr radius in A.

This allows considering the interval $r \in [r_{match} \geq 12, \infty)$ as possible for using the asymptotic potential $V_{as}(r)$ at large r and executing conventional calculations based on tabular values of $V(r)$ in the finite interval $r \in [r_1, r = 12]$ (Lesiuk et al., 2019). However, the above MEMO tabular values have been calculated in the unusually larger interval $r \in [r_1, r = 48]$ using special composite basis functions in different subintervals, taking into account both polarization and relativistic corrections DK-MRCI in the subinterval $r \in [r = 12, r = 48]$ (Mitin, 2011).

It is noted that the MEMO tabular values $r \in \{r_{41} = 6.5, ..., r_{48} = 11\}$ are smaller than the asymptotic ones by 5.5–6%, for $r = r_{51} = 14$ exceeding the asymptotic ones by 8%, and beyond the interval $r \in [r_{40} = 6.0, ..., r_{52} = 15]$ the difference is more than 10%. Based on this, we consider the case in which the potential $V(r)$ in the subintervals $r \in [r_{5k-4}, r_{5k+1}]$, $k = 1, ..., 9$ was approximated by the fifth-order interpolation Lagrange polynomials (LIPs) of the variable r in the interval $r \in [r_1, r_{46} = 14]$. In the subinterval, $r \in [r_e = r_{46} = 9.0, r_{match} = 14]$ we consider the approximation of the potential $V(r)$ by the fourth-order HIPs using the

values of the potential *V(r)* at the points $r \in \{r_e = r_{46} = 9.0,\ r_{47} = 10,\ r_{48} = 11\}$ and the values of the asymptotic potential $V_{as}(r)$ and its derivative $dV_{as}(r)/dr$ at the point $r = r_{match} = 14$. In the $r \in [r_{match} = 14, \infty)$ the potential *V (r)* is approximated by the asymptotic expansion (2) (Porsev & Derevianko, 2006). This approximation has been accepted in our paper (Gusev et al., 2019).

2.2. Algorithm for calculating scattering wave function of metastable states in KANTBP 4M program

To solve Eq. (1) for metastable states, we consider the boundary value problem (BVP) for the system of ordinary differential equations (ODE) of the second-order with respect to the unknown functions $\mathbf{\Phi}(z) = (\Phi_1(z)\ldots, \Phi_N(z))^T$ of the independent variable $z \in (z^{\min}, z^{\max})$ (Streng & Fics, 1977):

$$\left(-\frac{1}{f_B(z)}\mathbf{I}\frac{d}{dz} f_A(z)\frac{d}{dz} + \mathbf{V}(z) + \frac{f_A(z)}{f_B(z)}\mathbf{Q}(z)\frac{d}{dz} + \frac{1}{f_B(z)}\frac{d\ f_A(z)\mathbf{Q}(z)}{dz} - E\mathbf{I} \right)\mathbf{\Phi}(z) = 0 \tag{3}$$

Here $f_A(z) > 0$ and $f_B(z) > 0$ are continuous or piecewise continuous positive functions, **I** is the unit matrix, $\mathbf{V}(z)$ is a symmetric matrix ($V_{ij}(z) = V_{ji}(z)$), and $\mathbf{Q}(z)$ is an antisymmetric matrix ($Q_{ij} = -Q_{ji}$). These matrices have dimension $N \times N$ and their elements are continuous or piecewise continuous real or complex-valued coefficients from the Sobolev space $\mathcal{H}_2^{s\geq 1}(\Omega)$, providing the existence of nontrivial solutions subjected to homogeneous boundary conditions: Dirichlet (I kind) and/or Neumann (II kind) and/or third kind (III kind or the Robin condition) at the boundary points of the interval $z \in (z^{\min}, z^{\max})$ at given values of the elements of the real or complex-valued matrix $\mathcal{R}(z^t)$ of dimension $N \times N$.

(I): $\mathbf{\Phi}(z^t) = 0$, t=min and/or max (4)

(II): $\lim\limits_{z \to z^t} f_A(z)\left(\mathbf{I}\frac{d}{dz} - \mathbf{Q}(z) \right)\mathbf{\Phi}(z) = 0$, t=min and/or max (5)

(III): $\left(\mathbf{I}\frac{d}{dz} - \mathbf{Q}(z) \right)\mathbf{\Phi}(z)\Big|_{z=z^t} = R(z^t)\mathbf{\Phi}(z^t)$, t=min and/or max (6)

Eigenfunctions $\mathbf{\Phi}_m(z)$ obey the normalization and orthogonality conditions

$$\left(\mathbf{\Phi}_m \,|\, \mathbf{\Phi}_{m'}\right) = \int_{z_{\min}}^{z_{\max}} f_B \left(\mathbf{\Phi}_m(z)\right)^T \mathbf{\Phi}_{m'}(z)dz = \delta_{mm'}. \tag{7}$$

2.2.1. For the multichannel scattering problem

On the axis $z \in (-\infty, +\infty)$ at fixed energy $E = \Re E$, the desired matrix solutions $\mathbf{\Phi}(z) \equiv \{\mathbf{\Phi}_{\nu}^{(i)}(z)\}_{i=1}^{N}$, $\mathbf{\Phi}_{\nu}^{(i)}(z) = (\Phi_{1\nu}^{(i)}(z), \ldots, \Phi_{N\nu}^{(i)}(z))^{T}$ of the boundary problem (3) (the subscript ν means the initial direction of the incident wave from left to right $\rightarrow$ or from right to left $\leftarrow$) in the interval $z \in (z^{\min}, z^{\max})$. These matrices solutions are subjected to homogeneous third kind boundary conditions (6) at the boundary points of the interval $z \in (z^{\min}, z^{\max})$ with the asymptotes of the "*incident wave + outgoing waves*" type in open channels $i = 1, \ldots, N_o$ (Gusev et al., 2016):

$$\mathbf{\Phi}_{\rightarrow}(z \to \pm\infty) = \begin{cases} \mathbf{X}_{\min}^{(\rightarrow)}(z) + \mathbf{X}_{\min}^{(\leftarrow)}(z)\mathbf{R}_{\rightarrow} + \mathbf{X}_{\min}^{(c)}(z)\mathbf{R}_{\rightarrow}^{c}, & z \to -\infty, \\ \mathbf{X}_{\max}^{(\rightarrow)}(z)\mathbf{T}_{\rightarrow} + \mathbf{X}_{\max}^{(c)}(z)\mathbf{T}_{\rightarrow}^{c}, & z \to +\infty, \end{cases}$$
$$\mathbf{\Phi}_{\leftarrow}(z \to \pm\infty) = \begin{cases} \mathbf{X}_{\min}^{(\leftarrow)}(z)\mathbf{T}_{\leftarrow} + \mathbf{X}_{\min}^{(c)}(z)\mathbf{T}_{\leftarrow}^{c}, & z \to -\infty, \\ \mathbf{X}_{\max}^{(\leftarrow)}(z) + \mathbf{X}_{\max}^{(\rightarrow)}(z)\mathbf{R}_{\leftarrow} + \mathbf{X}_{\max}^{(c)}(z)\mathbf{R}_{\leftarrow}^{c}, & z \to +\infty, \end{cases} \tag{8}$$

Here $\mathbf{\Phi}_{\rightarrow}(z)$, $\mathbf{\Phi}_{\leftarrow}(z)$ are matrix solutions with dimensions $N \times N_o^L$, $N \times N_o^R$, where N_o^L, N_o^R are the numbers of open channels, $\mathbf{X}_{\min}^{(\rightarrow)}(z)$, $\mathbf{X}_{\min}^{(\leftarrow)}(z)$ are open channel asymptotic solutions at $z \to -\infty$, dimension $N \times N_o^L$, $\mathbf{X}_{\max}^{(\rightarrow)}(z)$, $\mathbf{X}_{\max}^{(\leftarrow)}(z)$ are open channel asymptotic solutions at $z \to +\infty$, dimension $N \times N_o^R$, $\mathbf{X}_{\min}^{(c)}(z)$, $\mathbf{X}_{\max}^{(c)}(z)$ are closed channel solutions, dimension $N \times (N - N_o^L)$, $N \times (N - N_o^R)$, $\mathbf{R}_{\rightarrow}, \mathbf{R}_{\leftarrow}$ are the reflection amplitude square

matrices of dimension $N_o^L \times N_o^L$, $N_o^R \times N_o^R$, $\mathbf{T}_{\rightarrow}, \mathbf{T}_{\leftarrow}$ are the transmission amplitude rectangular matrices of dimension $N_o^R \times N_o^L$, $N_o^L \times N_o^R$, $\mathbf{R}_{\rightarrow}^{c}, \mathbf{T}_{\rightarrow}^{c}, \mathbf{T}_{\leftarrow}^{c}, \mathbf{R}_{\leftarrow}^{c}$ are auxiliary matrices. For real-valued potentials $\mathbf{V}(z)$ and $\mathbf{Q}(z)$ the transmission $\mathbf{T}$ and reflection $\mathbf{R}$ amplitudes satisfy the relations:

$$\begin{aligned} &\mathbf{T}_{\rightarrow}^{+}\mathbf{T}_{\rightarrow} + \mathbf{R}_{\rightarrow}^{+}\mathbf{R}_{\rightarrow} = \mathbf{I}_{oo}, \quad \mathbf{T}_{\leftarrow}^{+}\mathbf{T}_{\leftarrow} + \mathbf{R}_{\leftarrow}^{+}\mathbf{R}_{\leftarrow} = \mathbf{I}_{oo}, \\ &\mathbf{T}_{\rightarrow}^{+}\mathbf{R}_{\leftarrow} + \mathbf{R}_{\rightarrow}^{+}\mathbf{T}_{\leftarrow} = \mathbf{0}, \quad \mathbf{R}_{\leftarrow}^{+}\mathbf{T}_{\rightarrow} + \mathbf{T}_{\leftarrow}^{+}\mathbf{R}_{\rightarrow} = \mathbf{0}, \\ &\mathbf{T}_{\rightarrow}^{T} = \mathbf{T}_{\leftarrow}, \quad \mathbf{R}_{\rightarrow}^{T} = \mathbf{R}_{\rightarrow}, \quad \mathbf{R}_{\leftarrow}^{T} = \mathbf{R}_{\leftarrow} \end{aligned} \tag{9}$$

ensuring unitarity and symmetry of **S**-scattering matrix:

$$\mathbf{S} = \begin{pmatrix} \mathbf{R}_{\rightarrow} & \mathbf{T}_{\leftarrow} \\ \mathbf{T}_{\rightarrow} & \mathbf{R}_{\leftarrow} \end{pmatrix}, \qquad \mathbf{S}^{+}\mathbf{S} = \mathbf{S}\mathbf{S}^{+} = \mathrm{I}. \tag{10}$$

Here symbols $^{+}$ and ^{T} denote conjugate transpose and transpose of a matrix, respectively.

2.2.2. For metastable states

With complex eigenvalues, $E = \Re E + i\Im E,\ \Im E < 0:\ \Re E_1 \le \Re E_2 \le ...$ the Robin BC follows from outgoing wave fundamental asymptotic solutions that correspond to Siegert outgoing wave BCs (Gusev et al., 2015).

For the set ODEs (1) with $f_A(z) = f_B(z) = 1,\ Q_{ij}(z) = 0$ and constant effective potentials

$V_{ij}(z) = V_{ij}^{L,R}$ in the asymptotic region, asymptotic solutions $\mathbf{X}_i^{(*)}(z \to \pm\infty)$ are expressed by the following formulas:

$$\begin{aligned}
&\mathbf{X}_{i_o}^{(\rightleftarrows)}(z \to \infty) \to \exp\left(+i\sqrt{E-\lambda_{i_o}^{L,R}}\,|z|\right)\boldsymbol{\psi}_{i_o}^{L,R},\ \lambda_{i_o}^{L,R} < \Re E,\ i_o = 1,...,N_o^{L,R},\\
&\mathbf{X}_{i_c}^{(c)}(z \to \infty) \to \exp\left(-\sqrt{\lambda_{i_c}^{L,R}-E}\,|z|\right)\boldsymbol{\psi}_{i_c}^{L,R},\ \lambda_{i_c}^{L,R} \ge \Re E,\ i_o = N_o^{L,R}+1,...,N.
\end{aligned} \tag{11}$$

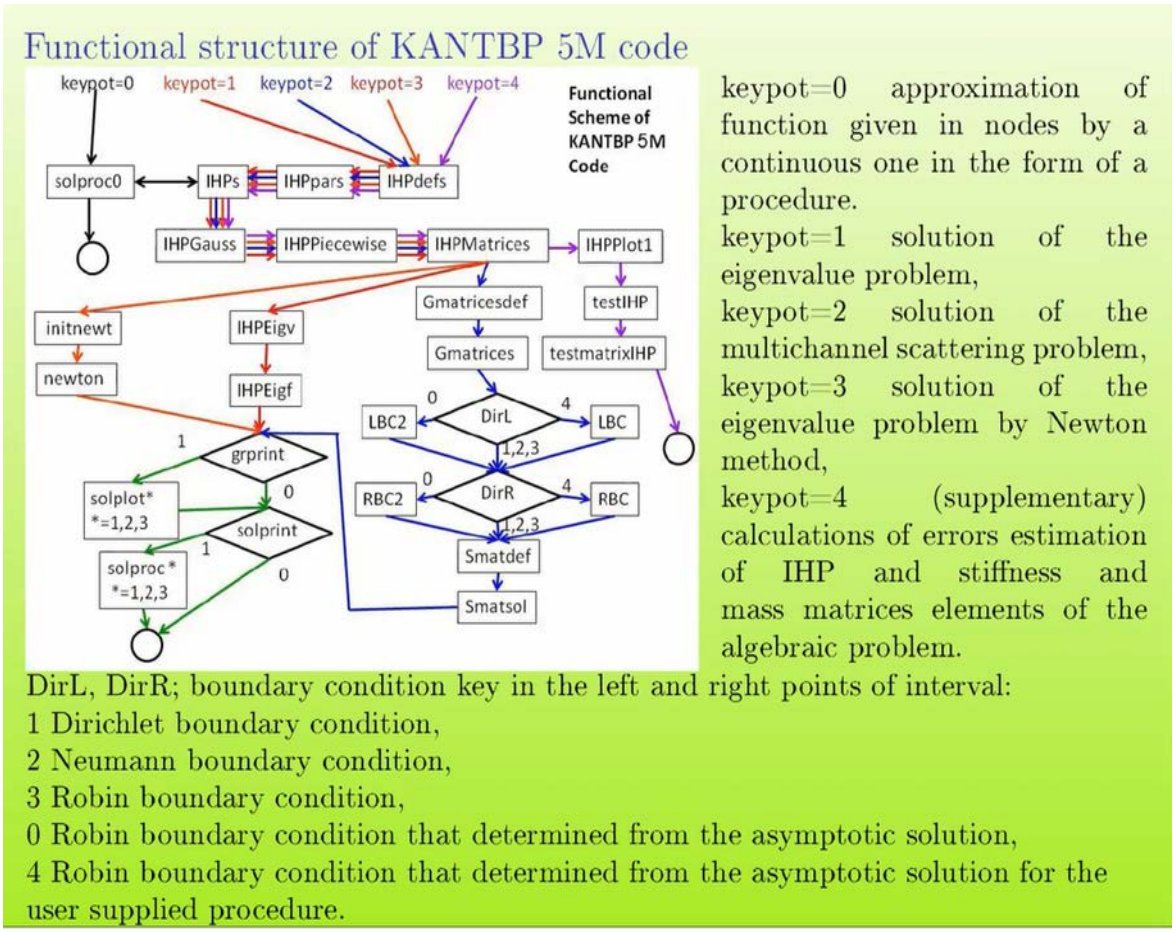

Fig.2. *Functional structure of KANTBP 4M code for different types of quantum problems*

Fig. 2 shows the functional structure of the KANTBP 4M code for different types of boundary quantum problems. It can be seen that for different values of *keypot*, there are different boundary problem types. For example, at *keypot* = 2, we have a solution of the multichannel scattering problem and at *keypot* = 3, we have a solution of the eigenvalue problem by the Newton method for calculating metastable states. *Dirl* and *DirR* are the boundary condition keys in the left and right points of the interval.

3. Calculation of scattering functions of metastable states

3.1. Calculation of resonance energies of metastable states

Firstly, we calculate resonance energies of metastable states at different values of the total angular momentum *L*. Using the KANTBP 4M program at *keypot* = 1 and *keypot* = 3, the mesh has been choosen as

$$\Omega = \left[1.90,\ 2.00,\ 2.15,\ 2.30,\ 2.42,\ 2.50,\ 2.62,\ 2.80,\ seq\left(3+0.25.i,\ i=\overline{0,11}\right),\right.$$
$$\left. seq\left(6+0.5.i,\ i=\overline{0,7}\right),\ seq\left(10+2.5.i,\ i=\overline{0,15}\right)\right]$$

with II kind boundary condition (Neumann condition) (5) at the left boundary point $r_1 = 1.90$ (*DirL* = 2) and III kind boundary condition (Robin condition) (6).

The numerical calculating results are presented in Tables 1 and 2. In these tables, the potential well minimum V_{Lmin} and maximum V_{Lmax}, the resonance energies E_{res} with real $\Re E_{\text{res}}$ and imaginary $\Im E_{\text{res}}$ parts for metastable states at different values of the total angular momentum *L* are calculated. It can be seen that all the imaginary $\Im E_{\text{res}}$ parts are negative of the order $(10^{-25} \div 0)$. For each value of $L < 23$, there is only one metastable state. On the other hand, for each value $L > 23$, there can be more than one metastable state. For example, at $L = 24$ or $L = 28$, there are two metastable states, and at $L = 30$ the number of metastable states is 3. At $L > 38$, there is only one metastable state for each value *L* and at $L > 47$, there are no energy levels in the well. Moreover, in these tables, the calculating results of resonance energies in other works are also presented in Slater-type orbitals (STO) (Koput, 2011; Lesiuk et al., 2019).

Table 1. *Resonance energies* $E_{\text{res}} = \Re E_{\text{res}} + i\Im E_{\text{res}}$ *(in* cm^{-1}*) of metastable states at different values of the total angular momentum L*

L	***v***	r_{min}	r_{max}	V_{Lmin}	V_{Lmax}	$\Re E_{\text{res}}$	$\Re E_{\text{res}}$ **(STO)**	$\Im E_{\text{res}}$	$\Im E_{\text{res}}$ **(STO)**
2		2.42	22.5	-920.72	0.04	0.079		$-9.635.10^{-3}$	
3	11	2.42	20.0	-916.89	0.10	0.095		$-9.635.10^{-3}$	
4		2.42	17.5	-911.78	0.21	0.504		$-5.147.10^{-4}$	
5		2.42	15.0	-905.39	0.39	0.504		$-5.147.10^{-4}$	

6		2.42	12.5	-897.72	0.70	0.504		$-5.147.10^{-4}$	
7	10	2.42	12.5	-888.78	1.03	0.504	0.972	$-5.147.10^{-4}$	$-5.6.10^{-3}$
8	10	2.42	12.5	-878.56	1.42	1.574	2.315	$-1.321.10^{-1}$	-0.149
9	10	2.42	10.0	-867.06	2.24	1.592	3.781	$-1.442.10^{-5}$	-0.499
10		2.42	10.0	-854.28	2.99	1.592		$-1.442.10^{-5}$	
11	9	2.42	9.5	-841.83	3.90	1.592	0.783	$-1.442.10^{-5}$	-1.10^{-5}
12	9	2.42	9.0	-827.46	5.02	4.053	0.352	$-2.950.10^{-2}$	-1.10^{-3}
13	9	2.50	9.0	-811.89	6.22	0.084	6.371	$-5,022.10^{-23}$	-0.543
14	8	2.50	8.5	-795.14	7.72	0.084		$-5,022.10^{-23}$	
15	9	2.50	8.5	-777.18	9.27	4.623	3.141	$-1.655.10^{-5}$	-1.10^{-5}
16	8	2.50	8.5	-758.02	11.25	9.096	7.705	$-1.887.10^{-2}$	-5.10^{-4}
17	8	2.50	8.0	-737.67	13.23	4.789	12.09	$-4,207.10^{-10}$	-0.032
18	7	2.50	7.5	-716.12	15.66	4.789	2.917	$-4,207.10^{-10}$	-1.10^{-5}
19	7	2.50	7.5	-693.37	18.18	11.527	9.637	$-1.491.10^{-4}$	-1.10^{-5}
20	6	2.50	7.5	-669.43	20.84	18.166	16.21	$-3.764.10^{-2}$	$-2.2.10^{-3}$
21	6	2.50	7.0	-644.29	24.15	6.403	4.200	$-5.186.10^{-13}$	-1.10^{-5}
22	6	2.50	7.0	-617.95	27.51	15.499	13.26	$-2.981.10^{-6}$	-1.10^{-5}
23	5	2.50	7.0	-590.42	31.02	24.465	22.220	$-3.392.10^{-3}$	$-2.5.10^{-4}$
24	5	2.50	7.0	-561.68	34.69	11.484	8.853	$-1,290.10^{-12}$	-1.10^{-5}
24	6	2.50	7.0	-561.68	34.69	33.184	30.74	-0.158	-0.037
25	4	2.50	6.5	-531.76	39.58	22.999	20.32	$-1.101.10^{-6}$	-1.10^{-5}

Fig. 3 shows the eigenfunctions $\Phi_{Lv}(r)$ of metastable states with complex energy values for a fixed value of the orbital momentum *L*. As can be seen from Fig. 1, these eigenfunctions have an increasing number of nodes localized inside the potential well ($0 < r < 10$) and outside the potential well , these eigenfunctions decrease to zero at $r \to +\infty$. i.e. metastable states of beryllium dimer exist only inside the potential well. It can be explained that with the growth of *L* the potential well minimum V_{Lmin} will increase and at $L > 39$. This minimum will exceed the dissociation threshold energy and then there will be no metastable state outside the potential well.

3.2. Calculation of scattering wave functions of metastable states

For calculating scattering wave functions of metastable states, we use the KANTBP 4M program at the *keypot* = 2 and the mesh has been choosen as

$$\Omega = \Big[1.90,\ 2.00,\ 2.15,\ 2.30,\ 2.42,\ 2.50,\ 2.62,\ 2.80,\ seq\left(3+0.25.i,\ i=\overline{0,11}\right),$$
$$seq\left(6+0.5.i,\ i=\overline{0,7}\right),\ seq\left(10+2.5.i,\ i=\overline{0,15}\right)\Big]$$

Table 2. *Resonance energies* $E(\text{res}) = \Re E(\text{res}) + i\Im E(\text{res})$ *(in* cm^{-1}*) of metastable states at different values of the total angular momentum L. Continuation of Table 1*

L	***v***	r_{min}	r_{max}	V_{Lmin}	V_{Lmax}	$\Re E_{\text{res}}$	$\Re E_{\text{res}}$ **(STO)**	$\Im E_{\text{res}}$	$\Im E_{\text{res}}$ **(STO)**
26	4	2.50	6.5	-500.63	44.18	7.996	4.773	$-1.257.10^{-20}$	-1.10^{-5}
26	5	2.50	6.5	-500.63	44.18	34.366	31.67	$-1.258.10^{-3}$	$-1.3.10^{-4}$
27	4	2.50	6.5	-468.31	48.96	22.032	18.779	$-1.765.10^{-10}$	-1.10^{-5}
27	5	2.50	6.5	-468.31	48.96	45.292	42.567	$-0.101.10^{-2}$	0.034
28	3	2.50	6.5	-434.78	53.92	6.963	3.009	$-6.232.10^{-27}$	-1.10^{-5}
28	4	2.50	6.5	-434.78	53.92	35.992	32.731	$-5.309.10^{-6}$	-1.10^{-5}
29	3	2.50	6.0	-400.07	60.55	23.517	19.452	$-2.229.10^{-13}$	-1.10^{-5}
29	4	2.50	6.0	-400.07	60.55	49.688	46.445	$-2.430.10^{-3}$	$-5.2.10^{-4}$
30	2	2.50	6.0	-364.15	66.79	11.354	7.180	0	-1.10^{-5}
30	3	2.50	6.0	-364.15	66.79	40.058	35.968	$-7.639.10^{-8}$	-1.10^{-5}
30	4	2.50	6.0	-364.15	66.79	62.792	59.548	$-1.254.10^{-5}$	-0.091
31	2	2.50	6.0	-327.04	73.23	32.621	28.549	$-4.357.10^{-13}$	-1.10^{-5}
31	3	2.50	6.0	-327.04	73.23	56.542	52.550	$-1.278.10^{-4}$	-1.10^{-5}
32	2	2.50	5.75	-288.73	80.67	52.660	48.671	$-8.935.10^{-8}$	-1.10^{-5}
32	3	2.50	5.75	-288.73	80.67	72.751	68.982	$-3.733.10^{-10}$	-0.013
33	1	2.50	5.75	-249.22	88.14	15.028	8.238	0	-1.10^{-5}
33	2	2.50	5.75	-249.22	88.14	71.134		$-2.398.10^{-9}$	
33	3	2.50	5.75	-249.22	88.14	88.035		$-8.887.10^{-12}$	
34	1	2.50	5.75	-208.52	95.83	47.784	40.779	$-1.401.10^{-14}$	-1.10^{-5}
35	1	2.50	3.50	-166.62	101.46	80.663	73.432	$-8.934.10^{-17}$	-1.10^{-5}
36	1	2.50	3.50	-123.52	123.44	113.474	105.338	$-9.959.10^{-14}$	$-7.1.10^{-3}$
37	0	2.50	3.50	-79.23	146.04	11.780	9.538	$-3.247.10^{-41}$	-1.10^{-5}
37	1	2.50	3.50	-79.23	146.04	45.893	135.737	$-1,129.10^{-14}$	-3.656
38	0	2.50	3.50	-33.73	169.25	53.592	51.2338	$-1.891.10^{-22}$	-1.10^{-5}
39	0	2.50	3.25	12.95	199.20	96.174	93.6727	$-6.656.10^{-25}$	-1.10^{-5}
40	0	2.50	3.25	60.83	227.53	139.477	136.795	$-9,895.10^{-22}$	-1.10^{-5}
41	0	2.62	3.25	102.56	256.58	183.435	180.520	$-1.591.10^{-18}$	$-1.2.10^{-3}$
42	0	2.62	3.25	148.34	286.33	227.964	224.726	$-6.748.10^{-17}$	-0.030
43	0	2.62	3.25	195.21	316.79	272.946	269.267	$-2.549.10^{-16}$	-0.173
44	0	2.62	3.25	243.17	347.96	318.196	314.016	$-8.911.10^{-17}$	-0.621
45	0	2.62	3.25	292.22	379.84	364.926	358.964	$-1.487.10^{-16}$	-1.622
46	0	2.62	3.0	342.36	419.21	411.060	403.449	$-1.593.10^{-16}$	-5.838
47	0	2.62	3.0	393.59	458.28	457.224	445.144	$-2.193.10^{-16}$	-6.238

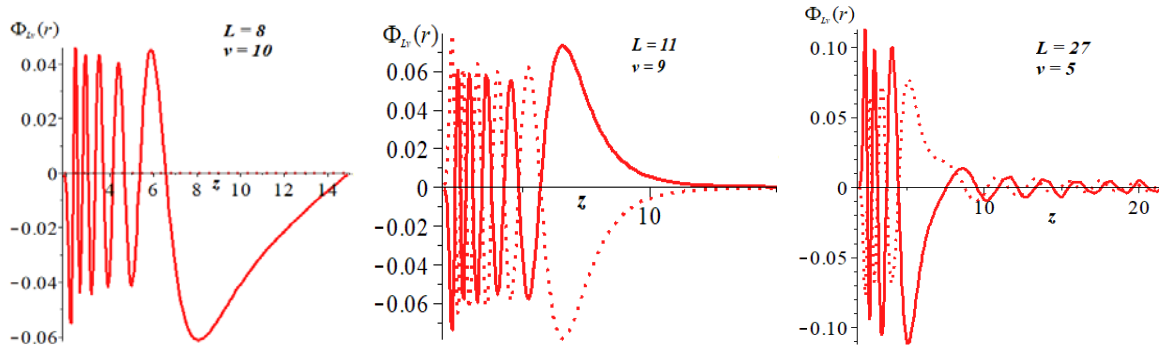

Fig. 3. *Plots of real (solid curve) and imaginary (dashed curve) parts of eigenfunctions* $\Phi_{Lv}(r)$ *of selected metastable states having eigenvalues from the table marked by L =8, 11, 27 with corresponding v =10, 9, 5*

with II kind boundary condition (Neumann condition) (5) at the left boundary point $r_1 = 1.90$ (*DirL* = 2) and III kind boundary condition (Robin condition) (6) at the right boundary point $r_{\max} = 50$ (*DirL* = 3) using the asymptotic formula (8) of the "*incident wave + outgoing waves*" type.

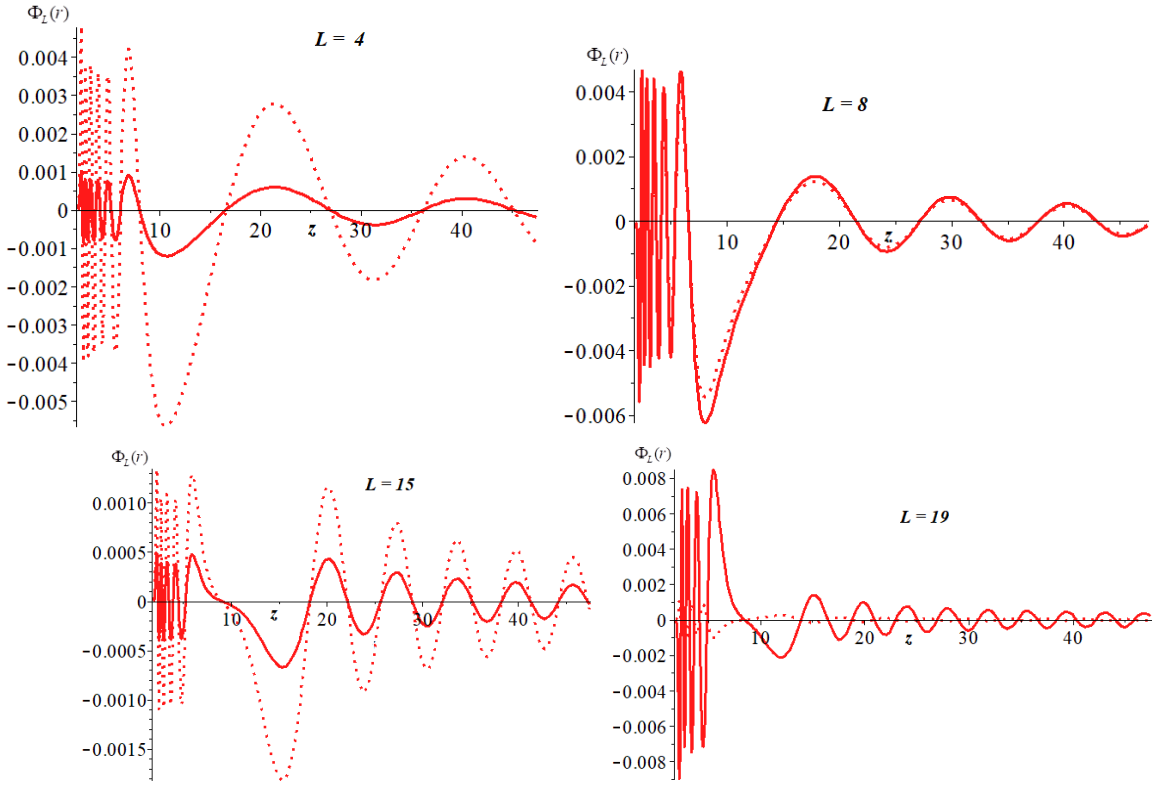

Fig.4. *Plots of the real (solid curves) and imaginary (dashed curves) parts of scattering wave functions* $\Phi_L(r)$ *for some selected metastable states in the vicinity of resonance energies* $\Re E_{\text{res}} \approx 0.504;\ 1.574;\ 4.623;\ 11.527$ *(in* cm^{-1}*) at corresponding values of the total angular momentum L= 4; 8; 15; 19*

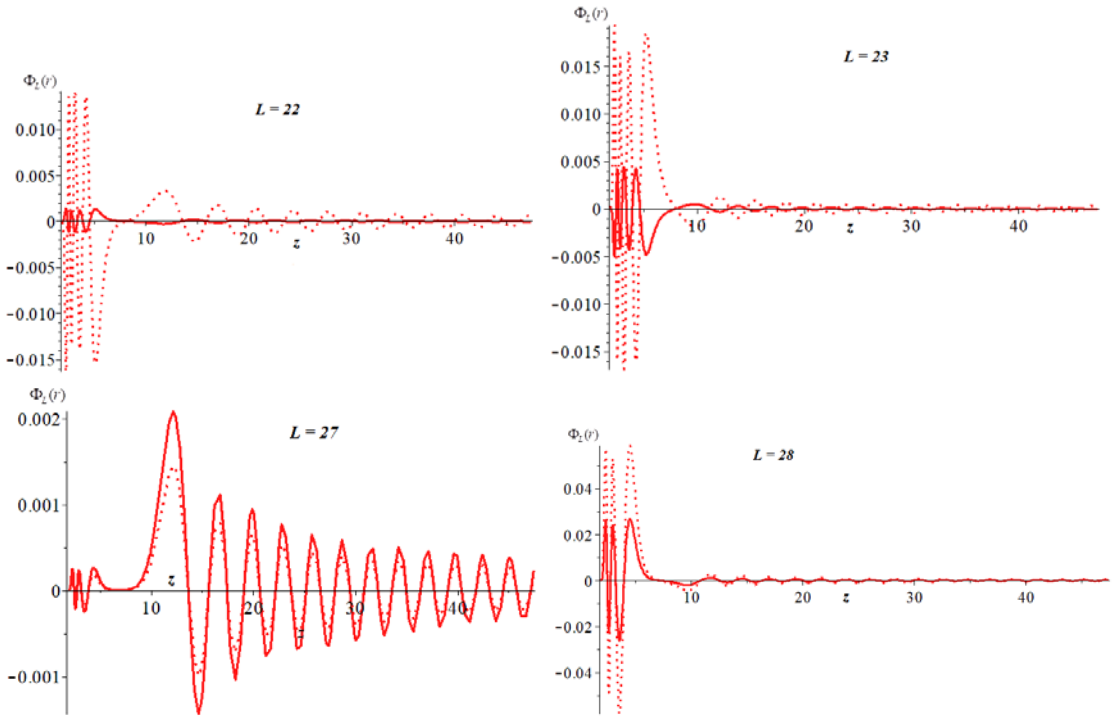

Fig.5. *Plots of the real (solid curves) and imaginary (dashed curves) parts of scattering wave functions $\Phi_L(r)$ for some selected metastable states in the vicinity of resonance energies $\Re E_{res} \approx$ 15.499; 24.465; 22.032; 35.992 (in cm^{-1}) at corresponding values of the total angular momentum L=22; 23; 27; 28*

The scattering **S**-matrix for some selected typical metastable states is calculated by using KANTBP 4M with formula (10) and is shown in Table 3. It can be seen that these matrices have complex elements with dimension 1*x*1.

Table 3. *Scattering **S**-matrix for some selected typical metastable states at corresponding resonance energies $\Re E_{res}$ (in cm^{-1}) and with corresponding values of the total angular momentum L*

L	$\Re E_{res}$	S-scattering matrix
4	0.504	[-0.912+0.408*i*]
8	1.574	[0.134+0.990*i*]
15	4.623	[-0.761+0.647*i*]
19	11.527	[0.971-0.236*i*]
22	15.499	[-0.985-0.167*i*]
23	24.465	[-0.872-0.489*i*]
27	22.032	[0.349-0.936*i*]
28	35.992	[-0.657+0.753*i*]

Fig. 4 and 5 show the real (solid curves) and imaginary (dashed curves) parts of scattering wave functions $\Phi_L(r)$ for metastable states at energies close to a very narrow resonance at different values of the total angular momentum *L*. As can be seen from Fig. 1, for the resonance energy, the scattering wave functions are seen to be localized within the

potential well ($0 < r < 10$). With the growth of L the nodes of scattering wave functions $\Phi_L(r)$ will decrease. It can be explained that inside the potential well (below the dissociation threshold) the number of metastable states decreases with an increase of L. On one hand, outside the potential well ($r > 10$) i.e. above the dissociation threshold with large of L, the metastable states disappear and the scattering wave functions will decrease exponentially. This means that the scattering of the diatomic beryllium molecule only occurs strongly in the potential well below the threshold energy i.e. in the interaction region between two atoms. To calculate scattering wave functions, we can calculate the transmission **T** and reflection **R** amplitudes. From that, we can also formulate BVP for calculating scattering wave functions for metastable states of beryllium trimer (triatomic molecule).

4. Conclusion

This paper presented a computational scheme and calculation results of scattering functions for metastable states of a diatomic beryllium molecule in laser spectroscopy. The efficacy of the applied approach and program is demonstrated by the approximation of the tabulated potential function in a finite interval and its extension beyond this interval using asymptotic expansions and its matching via interpolation Hermite polynomials and modeling calculations of the rotational vibrational spectrum of narrow-band metastable states with complex-valued energy eigenvalues. For selected metastable states the corresponding scattering states with real-values resonance energies are calculated and shown in graphs.

These results have significant importance for further experiments in laser spectroscopy of the beryllium dimer. It is also important for modeling a near-surface diffusion of the beryllium dimers in connection with the well-known multifunctional use of beryllium alloys in modern technologies of the electronic, space, and nuclear industries.

In the future based on these results and the presented FEM program, we can develop this implementation for the calculation of scattering wave functions for metastable states of beryllium trimer (triatomic molecule) and waveguide problems by solving the eigenvalue and scattering problems in the closed coupled channel method for high-precision laser spectroscopy.

❖ ***Conflict of Interest:*** *Authors have no conflict of interest to declare.*

❖ ***Acknowledgements.*** *The work was supported by the Ho Chi Minh City University of Education (Grant CS.2020.19.47).*

REFERENCES

Derbov, V. L., Chuluunbaatar, G., Gusev, A. A., Chuluunbaatar, O., Vinitsky, S. I., Gozdz, A., Krassovitskiy, P. M., & Mitin, A. V. (2020). On calculations of metastable and Rydberg states of diatomic beryllium molecule and antiprotonic helium atom. *In: Proc. of SPIE*., 11458, 114580.

Derbov, V. L., Chuluunbaatar, G., Gusev, A. A., Chuluunbaatar, O., Vinitsky, S. I., Gozdz, A., Krassovitskiy, P. M., Filikhin, I., & Mitin, A. V. (2021). Spectrum of beryllium dimer in ground $X^1\Sigma^+_g$ state. *J. Quant. Spectrosc. Radiat. Transf*, 262, 107529–1-10.

Gusev, A., Vinitsky, S., Gerdt, V., Chuluunbaatar, O., Chuluunbaatar, G., Hai L. L., & Zima, E. (2021). A maple implementation of the finite element method for solving boundary problems of the systems of ordinary second order differential equations. *Springer Nature Switzerland AG. CCIS.*, (1414), 152-166.

Gusev, A. A., Luong, L. L., Chuluunbaatar, O., Vinitsky S. I., KANTBP 4M – program for solving boundary problems of the self-adjoint system of ordinary second order differential equations. JINRLIB; 2015. Retrieved from http://wwwinfo.jinr.ru/programs/jinrlib/kantbp4m/indexe

Gusev, A., Chuluunbaatar, O., Vinitsky, S., Derbov, V. L., Gozdz, A., Krassovitskiy, P. M., Filikhin, I., Mitin A. V., Luong, L., H., & Tran, T., L. (2019). On rotational-vibrational spectrum of diatomic beryllium molecule. *In: Proceedings of SPIE., 11066*(1), 1106619.

Gusev, A. A., Gerdt, V. P., Luong L. H., Derbov, V. L., Vinitsky, S. I. & Chuluunbaatar, O. (2016). Symbolic-Numeric Algorithms for Solving BVPs for a System of ODEs of the Second Order: Multichannel Scattering and Eigenvalue Problems. *CASC, Springer International Publishing Switzerland, LNCS., 9890*(1), 212-227.

Gusev, A. A., Luong, L., H., Chuluunbaatar, O., Ulziibayar, V., Vinitsky, S. I., Derbov, V. L., Gozdz, A., & Rostovtsev, V. A. (2015). Symbolic-numeric solution of boundary-value problems for the Schrodinger equation using the finite element method: scattering problem and resonance states. *CASC, Springer International Publishing Switzerland, LNCS., 9301*(1), 182-197.

Koput, J. (2011). The ground-state potential energy function of a beryllium dimer determined using the single-reference coupled-cluster approach. *PCCP., 13*(45), 20311.

Lesiuk, M., Przybytek, M., Balcerzak, J. G., Musial, M., & Moszynski, R. (2019). Ab initio potential energy curve for the ground state of beryllium dimer. *J. Chem. Theory Comput*, (15), 2470-2480.

Merritt, J. M., Bondybey, V. E., & Heaven, M. C. (2009). Beryllium dimer caught in the act of bonding. *Science, 324*(5934), 1548-1551.

Meshkov, V. V., Stolyarov, A. V., Heaven, M. C., Haugen, C., & LeRoy, R. J. (2014). Direct-potential-fit analyses yield improved empirical potentials for the ground $X^1\,\sigma_g{}^+$ state of Be_2. *J. Chem. Phys., 6*(140), 064315.

Mitin, A. V. (2011). Ab initio calculations of weakly bonded He_2 and Be_2 molecules by MRCI method with pseudonatural molecular orbitals. *Int. J. Quantum Chem.,* (111), 2560-2567.

Mitin, A. V. (2017). Unusual chemical bonding in the beryllium dimer and its twelve vibrational levels. *Chem Phys Lett.,* (682), 30-3.

NIST. Physical Measurement Laboratory. *Atomic spectroscopy databases.* Retrieved from https://www.nist.gov/pml/atomic-spectroscopy-databases

Patkowski, K., Spirko, V., & Szalewicz, K. (2009). On the elusive twelfth vibrational state of beryllium dimer. *Science*, (326), 1382-1384.

Porsev, S. G., & Derevianko, A. (2006). High-accuracy calculations of dipole, quadrupole, and octupole electric dynamic polarizabilities and van der Waals coefficients C_6, C_8, and C_{10} for alkaline-earth dimers. *JETP*., (102), 195-205.

Sheng, X. W., Kuang, X. Y., Li, P., & Tang, K. T. (2013). Analyzing and modeling the interaction potential of the ground-state beryllium dimer. *Phys. Rev*. A, (88), 022517.

Streng, G., & Fics, G. (1977). *Theory of finite element method*. Moscow: World.

TÍNH TOÁN HÀM SÓNG TÁN XẠ ỨNG VỚI CÁC TRẠNG THÁI SIÊU BỀN CỦA PHÂN TỬ LƯỠNG NGUYÊN TỬ BERYLI

Lương Lê Hải[1*], Nguyễn Minh Nhựt[1], Lưu Kim Liên[1], Gusev Alexander Alexandrovich[2]

[1]Trường Đại học Sư phạm Thành phố Hồ Chí Minh, Việt Nam

[2]Viện Liên hiệp Nghiên cứu Hạt nhân Dubna, Thành phố Dubna, Liên bang Nga

[*]Tác giả liên hệ: Lương Lê Hải – Email: haill@hcmue.edu.vn

Ngày nhận bài: 23-9-2021; ngày nhận bài sửa: 09-11-2021; ngày chấp nhận đăng: 08-12-2021

TÓM TẮT

Trong bài báo này chúng tôi trình bày sơ đồ thuật toán và kết quả tính toán hàm sóng tán xạ đối với các trạng thái siêu bền của phân tử lưỡng nguyên tử Beryli trong quang phổ laser. Nghiệm của bài toán biên được tính toán bằng chương trình phần mềm được biên soạn bởi tác giả bài báo cùng các cộng sự khoa học ở Viện Liên hiệp Nghiên cứu Hạt nhân Dubna, Thành phố Dubna, Liên bang Nga. Các thuật toán của chương trình tính toán này dựa trên phương pháp phần tử hữu hạn với độ chính xác cao. Hàm thế năng được cho ở dạng bảng giá trị được nối với hàm thế năng tiệm cận Waals bằng cách sử dụng đa thức nội suy Hermite và đảm bảo tính liên tục của nghiệm hàm cùng đạo hàm của nó. Sự hiệu quả của chương trình tính toán này được thể hiện bằng việc tính toán các giá trị năng lượng cộng hưởng ở dạng phức của các trạng thái siêu bền trong phổ xung động quay của phân tử lưỡng nguyên tử Beryli. Với các trạng thái siêu bền này, các hàm sóng tán xạ tương ứng với năng lượng cộng hưởng mang giá trị thực được tính toán và biểu diễn dưới dạng đồ thị.

Từ khóa: bài toán tán xạ; chương trình KANTBP 4M; phân tử lưỡng nguyên tử beryli; phương pháp phần tử hữu hạn; trạng thái siêu bền